Carbon sequestration by enhanced weathering of basalt and its applicability

A thesis submitted in partial fulfilment of the
requirements for the M.Sc. degree programme

by

Debasish Maji

20236401

Indian Institute of Science Education and Research, Pune

April, 2025

under the guidance of

Dr. Gyana Ranjan Tripathy

Earth and Climate Science Department

IISER Pune

Certificate

This is to certify that this dissertation entitled “Carbon sequestration by enhanced weathering of basalt and its applicability” towards the partial fulfilment of the M.Sc. degree programme at the Indian Institute of Science Education and Research, Pune represents study carried out by **Debasish Maji** at IISER Pune under the supervision of **Dr. Gyana Ranjan Tripathy**, Associate Professor, Department of Earth and Climate Sciences, during the academic year 2024-2025.

Debasish Maji
(M.Sc. Student)

Dr. Gyana Ranjan Tripathy
(Supervisor)

This thesis is dedicated to my parents

Declaration

I hereby declare that this dissertation titled “Carbon sequestration by enhanced weathering of basalt and its applicability” submitted for the M.Sc. degree program at the Indian Institute of Science Education and Research, Pune is my original work under the supervision of Dr. Gyana Ranjan Tripathy. All sources used in this dissertation have been duly acknowledged and cited by academic conventions and guidelines. Any assistance received during the research and writing process has been acknowledged appropriately. No part of this dissertation has been submitted for any other degree or qualification at any other institution.

Debasish Maji
(M.Sc. Student)

Dr. Gyana Ranjan Tripathy
(Supervisor)

Acknowledgments

I am deeply grateful to all those who, in various ways, contributed to the successful completion of this dissertation. First, I would like to express my profound thanks to my mentor, **Dr. Gyana Ranjan Tripathy**, for his support and direction as well as for setting up the required funds for the field trip for my dissertation. I am deeply indebted to **Dr. Shilpa Patil Pallai** for her guidance during the rock sampling field. I also thank **Ms. Kruttika Mohapatra** and **Ms. Subhashree Maity** for their help during the field trip. I am especially thankful to **Mr. Rakesh Kumar Rout**, my senior in the laboratory, whose constant encouragement and insightful advice played a crucial role throughout the research. I would also like to thank **Mr. Vikrant Bartakke** and **Mr. Achyuth Venugopal** for their consistent help during the analysis phase, which made the entire process much smoother. I would like to extend a sense of gratitude to my **Parents** for their sacrifices, encouragement, love, and support. Finally, I would like to thank all my **friends** and **colleagues** for their support.

Table of Contents

List of Abbreviations

GHG: Greenhouse Gas

CCS: Carbon Capture & Storage

EOR: Enhanced Oil Recovery

EGR: Enhanced Gas Recovery

EW: Enhanced Weathering

DVP: Deccan Volcanic Province

K-Pg: Cretaceous-Paleogene

LOI: Loss on Ignition

XRF: X-ray Fluorescence

TAS: Total Alkali-Silica

AFM: Alkali-FeO*-MgO

List of Figures

List of Tables

Abstract

Several physical and chemical geoengineering pathways have been proposed to tackle the Anthropocene rise in atmospheric CO_2 and hence, global warming. Among these, enhanced weathering of mafic and ultramafic rocks has been proposed as a carbon sequestration method to mitigate climate change. This mechanism is motivated by carbonic acid-mediated weathering of silicate minerals, which serves as the natural sink for CO_2 over million-year timescales. This work is an attempt to study the efficiency of enhanced weathering of basalt, particularly subalkaline tholeiitic basalt, as it is the major rock type of the Deccan Trap, one of the most voluminous large igneous provinces. Towards this, a lab-controlled experiment involving the interaction of basalt powder (grain size: < 150 μm) with deionized water (pH ≈ 5.8 ± 0.2) for different time intervals (1 hour, 6 hours, 12 hours, 24 hours, and 48 hours) was carried out to accurately quantify the carbon sequestration potential of powdered basalt without any background interferences. Notably, a progressive increment of total alkalinity, silica, and major cations (Na^+, Ca^{2+}, Mg^{2+}) in the reacting medium was observed with time. Results from the experiment suggest that 1 g of basalt powder has the potential to sequester 0.280 ± 0.085 mg of CO_2 within 24 hours, and the relative mobility of elements is $Na^+ > Ca^{2+} > Mg^{2+}$ during this short-term (hourly-scale) weathering interaction. It demonstrates that basalt dust significantly increases the weathering rate of silicate minerals and hence may facilitate sequestration of atmospheric CO_2 by increasing the alkalinity of water, which is stable for approximately one million years in the hydrological cycle.

1. Chapter - 1

1.1 Introduction

CO_2 is a greenhouse gas, which plays an important role in regulating Earth's temperature. Over the last few years, it has become the predominant contributor to overall GHG emissions (Voormeij & Simandl, 2004). Anthropogenic impact (mainly, burning of fossil fuels and biomass) on the global carbon cycle has caused a sharp rise in the concentration of CO_2 in the atmosphere, which is a major contributing factor to the observed global warming (IPCC, 2007). Fossil fuels provide more than 85% of the energy needs of the world (Mun & Cho, 2013); as a result, the atmospheric CO_2 concentration has been rising at a rate of 2 ppm per year on average since 2000 (Brierley & Kingsford, 2009). To remove excess CO_2 from the atmosphere, significant efforts have been undertaken to develop resource-efficient technologies and green technologies. Even though these strategies to lower CO_2 emissions have gained popularity in recent years, there is still a potential requirement of managing CO_2 emissions on a large scale. This is where CCS technology is needed (IPCC, 2005). CCS technology describes the process of capturing, separating, transporting, and storing CO_2.

Approximately 40% of carbon emissions are absorbed by different carbon sinks, with the other 60% remaining in the atmosphere (Saran et al., 2017). There are three primary categories of practical carbon storage sites, and each has unique constraints, longevity, and associated costs. These storage options are categorized into geological, mineralogical, and ocean-based methods (Rigopoulos et al., 2015). Out of these three, mineral storage has the highest capacity to sequester CO_2, surpassing the total amount released from the oxidation of all fossil fuel reserves worldwide (Sanna et al., 2014). This makes it an extremely efficient way to capture and store all of the current CO_2 emissions.

1.2 Techniques of CO_2 Sequestration

1.2.1 Geological Sequestration

Geological sequestration involves absorbing CO_2 and storing it deep inside geological formations to prevent it from entering the atmosphere and causing climate change. Saline aquifers, underground salt caverns, deep coal seams, and depleted oil & gas fields are potential locations where geological sequestration is possible.

Fossil fuel reserves, both active and depleted, are suitable subterranean formations for storing CO_2 (Gentzis, 2000). The processes of enhanced oil recovery (EOR) and enhanced gas recovery

(EGR) can also be improved by injecting CO_2 into these reservoirs. This procedure is a method that is economically appealing since it can boost oil recovery by up to 50% and gas recovery by up to 15% in active fields (Saran et al., 2017). The estimated capacity for storing CO_2 is 140 Gt for depleted gas reservoirs, 40 Gt for depleted oil reservoirs, and 65 Gt CO_2 can be stored through the process of EOR globally (Huijgen & Comans, 2003). As gas reservoirs contain a very little amount of water, they have a larger storage capacity for storing CO_2 than oil reservoirs and this capacity can almost exactly match the volume of extracted gas (Holloway, 2005). The existence of subsurface water, the distance from CO_2 emission sites, and the possibility of leakage are the three primary elements that affect how efficiently CCS works in these settings (Park, 2005). The possibility of leaking CO_2 due to instability of the subsurface conditions is a serious worry with this approach. To reduce these hazards and guarantee environmental efficacy and safety, continuous monitoring is necessary (Doria, 2022).

Fractures in deep coal seams (cleats) can efficiently capture CO_2, making them a reliable choice for long-term CO_2 storage. According to the IEA Greenhouse Gas R&D Programme, 2001, deep un-mineable coal seams have the capacity of storing 15 Gt. of CO_2 globally. Also, injection of CO_2 within coal seams improves coal-bed methane recovery by increasing the temperature and pressure (Gunter et al., 2005).

Deep saline aquifers are underground rock formations that contain extremely salty water which is unfit for drinking or farming. These formations are suitable for storing CO_2. But only a little percentage of their whole volume, roughly 2%, is useful for this (Voormeij & Simandl, 2004). On a global scale, it is estimated that these aquifers have the capacity to store approximately 100 Gt. of CO_2 (Huijgen & Comans, 2003). Due to the differences in density and viscosity between CO_2 and the aquifer water, injected CO_2 tends to rise and spread out beneath the cap rock (Gale, 2004). There is a chance that CO_2 stored in these aquifers can be leaked, particularly if the cap rock has cracks.

By dissolving subterranean salt beds with water and extracting the salt as brine, salt caverns offer a very safe way to store CO_2 since inherent impermeability of salt serves as a strong barrier against leaks (Doria, 2022; Voormeij & Simandl, 2004). Nevertheless, the environmental effects of brine disposal and the associated high costs provide two significant obstacles to this approach (Saran et al., 2017). As a result, salt caverns are not frequently used or regarded as a suitable storage option.

1.2.2 Ocean Sequestration

The ocean serves as the biggest sink for CO_2 emissions; it has greater potential for CO_2 storage than both geological and mineral processes combined (Gentzis, 2000). Naturally, a significant amount of atmospheric CO_2 is absorbed by the ocean, which keeps the ratio of the equilibrium concentration of CO_2 between the atmosphere and ocean roughly at 1:4 (Saran et al., 2017). Currently, oceans are removing roughly 6 Gt. of CO_2 per year from the atmosphere, but there is always a chance that CO_2 will eventually return to the atmosphere, as oceans may store CO_2 for up to 500 years (Voormeij & Simandl, 2004); therefore, this approach is not permanent. Injection of CO_2 below 1500 meters contributes to more stable and long-lasting storage (Ozaki et al., 2001). The procedure is less precise as CO_2 tends to rise before dissolving since it is less dense than seawater. Although injecting in the deeper level can lower this danger, it requires more sophisticated technology, which raises the price.

An alternative ocean sequestration method involves injecting CO_2 at depths greater than 3000 meters. At such depths, the combination of high pressure and low temperatures makes CO_2 react with ocean water, and it forms a compound called clathrate, a structure made up of about six water molecules for every CO_2 molecule (Sloan, 2003). These denser CO_2 hydrates sink and settle on the ocean floor (Voormeij and Simandl, 2004). But these hydrates are also not permanently stable, and this process can disrupt ocean chemistry and negatively impact marine life (Saran et al., 2017).

1.2.3 Mineral Sequestration

Geological sequestration provides a limited amount of space for CO_2 to be sequestered, and it requires long-term monitoring to prevent leakages. For ocean sequestration, longevity and technological barriers are major disadvantages. Due to these reasons, mineral sequestration stands as a more reliable option for capturing CO_2. This method can absorb more carbon than the entire amount released by the oxidation of fossil fuel reserves worldwide (Huijgen and Comans, 2003).

It has been observed that one of the main processes affecting the long-term decrease of atmospheric CO_2 is the chemical weathering of silicate minerals (Holland et al., 1986). The current natural silicate weathering-induced CO_2 drawdown is around 90 - 140 MtC per year (Hilton & West, 2020). The process begins with atmospheric CO_2 dissolving in rainwater to form carbonic acid (H_2CO_3), which has a pH of roughly 5.6. Although it is a very weak acid, it can dissolve silicate rocks over extended periods of time (Berner et al., 1983). Dissolved ions

are released into water by these rocks as they get weathered. Ca^{2+} and Mg^{2+} released during this process combine with the carbonate or bicarbonate ions to form $CaCO_3$ and $CaMg(CO_3)_2$ in the ocean. These limestones and dolomites can trap CO_2 for millions of years (Schuiling & Krijgsman, 2006).

$$(Ca, Mg, Na, K) - silicates + CO_2 + H_2O \rightarrow Cations\ (Ca^{2+}, Mg^{2+}, Na^{+}, K^{+}) + HCO_3^{-} + H_4SiO_4$$

$$Cations\ (Ca^{2+}, Mg^{2+}, Na^{+}, K^{+}) + HCO_3^{-} \rightarrow Carbonates + CO_2 + H_2O$$

This naturally occurring weathering cycle is a very slow process. To counter global climate change, several scientists have suggested speeding up the process of naturally occurring chemical weathering (Taylor et al., 2016; Schuiling & De Boer, 2011; Schuiling & Krijgsman, 2006). By distributing finely powdered silicate rocks across different land types, such as agricultural or forested regions, enhanced weathering (EW) is a geoengineering tool that can be used to capture atmospheric CO_2 (Seifritz, 1990; Schuiling & Krijgsman, 2006). Minerals present in this rock powder react with atmospheric CO_2 and H_2O to produce dissolved CO_3^{2-} or HCO_3^{-} ions, which may remain on land by forming solid minerals or can be carried by rivers to the ocean, where they may dissolve or precipitate out by forming calcium carbonate (Archer et al., 1997). In this way, EW increases the rate of the naturally occurring silicate weathering cycle (Knapp et al., 2023).

The focus of EW has been on mafic and ultramafic rocks due to their very fast dissolution kinetics (Hartmann et al., 2013). The higher olivine content of ultramafic rocks causes them to weather more quickly than mafic rocks. But ultramafic rocks (mainly, peridotite) are mostly found in ophiolitic complexes, whereas mafic rocks (mainly, basalt) are more readily found at the Earth's surface. Another key disadvantage with ultramafic rocks is that olivine contains Ni, a potentially hazardous element that poses a major threat to marine ecosystems (Schuiling & Krijgsman, 2006; Zhang et al., 2024). Therefore, basalt is a superior choice for EW than olivine-rich rocks (Vienne et al., 2022).

There is a wide range of carbon sequestration potentials reported by recent studies for basalt, ranging from 13 to 73 kg of equivalent CO_2 per tonne of rock used for EW per year (Honvault et al., 2024). Also, EW of basalt on agricultural lands or forest regions tends to improve the quality of soil by increasing pH and cation exchange capacity by up to 20%–87% (Anda et al., 2013; Swoboda et al., 2022; Honvault et al., 2024) and reducing N losses by up to 55% (Amann et al., 2020; Swoboda et al., 2022). This method simultaneously increases Mg availability by 100%-800% (Amann et al., 2020; Kelland et al., 2020; Honvault et al., 2024), increases K

availability by 1%-10% (Renforth et al., 2015; Swoboda et al., 2022; Honvault et al., 2024), and protects crops from diseases by improving Si availability up to 180% (Luyckx et al., 2017; Berge et al., 2012; Honvault et al., 2024). In addition, adverse effects of EW of basalt through the release of trace metals can be reduced via the application of biochar with it. It has been observed that adding biochar with basalt powder significantly reduces the intake of trace elements within plants by 44%. (Natasha et al., 2022).

According to multiple studies, using basalt dust as fertilizer can cut the need for chemical fertilizers by up to 50%, which results in significant cost savings (Conceição et al., 2022). The amount of basalt dust required for soil amendment varies from 1 to 10 tons per hectare, depending on the quality of the land (Richardson, 2024). This process will cost about $50 to capture one ton of CO_2, which is far less than direct air capture and a few other methods.

1.3 Objective of the Thesis

The main objective of this thesis is –

- To evaluate the efficacy of powdered basalt in consuming atmospheric CO_2.
- To examine the cations released during enhanced weathering to the hydrological cycle.

Mainly, the Deccan Volcanic Province has been the focus of this experiment. If proven reliable, India's large flood basalts would offer an extra alternative for mineral sequestration in areas where traditional geological storage options are limited.

1.4 Structure of the Thesis

The overall thesis can be divided into four main chapters –

- **Chapter 1** – It briefly introduces the mechanism behind enhanced weathering and how it can help to mitigate climate change. It also summarises the benefits of its application in the agricultural field.
- **Chapter 2** – This chapter provides detailed analytical protocol that has been followed during the analyses of the rock samples and controlled experiment.
- **Chapter 3** – It is further divided into two subsections: (i) Results – all the outcomes from the analyses have been described, and (ii) Discussion – interpretation of the major observation from the data obtained from the series of experiments.
- **Chapter 4** – Summarizes all the work that has been achieved, the major findings, and related interpretations.

2. Chapter – 2

2.1 Sampling

Figure 4: Location map of the sampling site from Deccan Trap, India

The Deccan Volcanic Province is extensively studied because of its connections to deep mantle-derived volcanism, crustal uplift, changes in biodiversity, past climate fluctuations, and the breakup of the southern Gondwana supercontinent (Courtillot, 1990; Khosla & Sahni, 2003). Near the K-Pg boundary, DVP underwent a major eruption of tholeiitic basalt, making it one of the most voluminous large igneous provinces (Chenet et al., 2009). The DVP spans more than 500,000 km² across various portions of northwest, central, and southern India. According to studies, it might possibly lie beneath the Arabian Sea for an extra 1,000,000 km² (Sen et al., 2001; Jay & Widdowson, 2008). Lava flows of this igneous province vary greatly in thickness throughout the region, ranging from less than 200 m in the east to up to 1.5 to 2 km in the west (Colleps et al., 2021).

Deccan basalt is predominantly tholeiitic in nature, which contain minerals like clinopyroxene, olivine, plagioclase feldspar, opaque phases, and altered volcanic glass (Beane et al., 1986; Kale et al., 2020). Stratigraphic studies, geochemical analysis, and paleomagnetic data confirm that DVP is divided into twelve formations and three subgroups (Verma & Khosla, 2019).

For this study, 30 rock samples were collected from Katraj Ghat, Pune (18°25'22.4"N, 73°49'51.3"E). The area falls in the uppermost flow region of the Poladpur Formation. Multiple tholeiitic basalt flows with columnar joints have been mapped here (Beane et al., 1986; Kale et al., 2020).

2.2 Geochemical Analyses

2.2.1 Major Oxides

Rock samples were powdered using Retsch PM 100, a planetary ball milling machine equipped with agate grinding jars and balls. Powder of each sample was sieved using nylon mesh cloth with 100 mesh size. The loss on ignition (LOI) for these samples were estimated by monitoring the weight loss during sample combustion at 950°C. To prepare the XRF fusion bead, an approximately 0.55g sample was mixed with 9.35g of flux (67% lithium metaborate, 33% lithium tetraborate), and a few drops of 2% anhydrous lithium bromide were added. Fusion beads were prepared at 1100°C in a platinum crucible. Concentrations of the major oxides in the rock powders were measured using an XRF spectrometer (Bruker S8 Tiger) with an accuracy of 2 % and precision of 1%, respectively.

2.2.2 Controlled Experiment

Based on the data of major oxides, five samples that were good representatives of tholeiitic basalt were selected for the controlled experiment. 0.5g of each sample with a grain size of < 150 μm was taken with 35 mL of Milli-Q water in a 50 mL centrifuge tube. These centrifuge tubes were shaken at 50 rpm to simulate natural agitation. Before starting the experiment, the pH of Milli-Q water was also measured.

For each rock sample, this experiment was done for 1 hour, 6 hours, 12 hours, 24 hours, and 48 hours, respectively, to monitor the changes in solution chemistry with time. These samples were immediately centrifuged at 3000 rpm for 30 minutes after the shaking was done for each time point, and then the supernatant was filtered through a 0.22 μm nylon syringe filter.

For every filtered leachate water sample, two distinct aliquots were prepared. To measure the concentration of major cations, one aliquot was acidified with 6N HNO_3 to bring the pH of the

sample down to 2, while the other aliquot was left unacidified to measure the concentration of major anions.

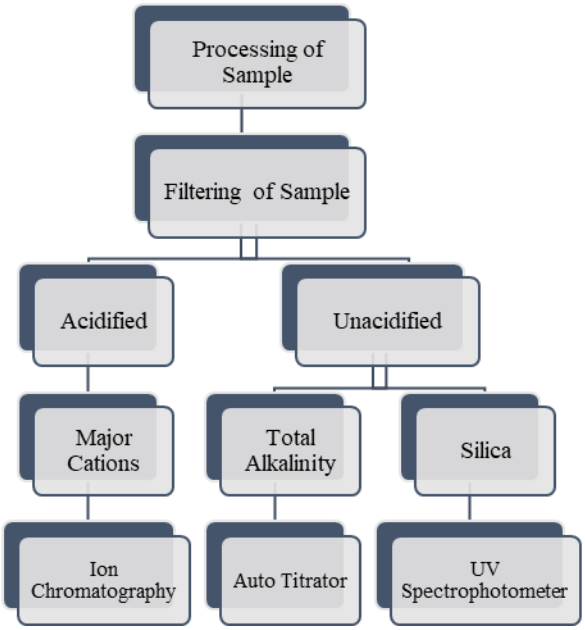

Figure 5: Flowchart of analytical techniques followed in this study

2.2.2.1 Total Alkalinity

The alkalinity of the samples was measured by using the Metrohm Titrino Plus 877 auto-titrator through acid-base titration with 0.01N HCl. The probe of the instrument was calibrated by using standard buffer solutions with pH values of 4.0, 7.0, and 9.2 before the analysis. The average accuracy for the analysis was 1% with an average precision of 1%.

2.2.2.2 Major Ions

Ion Chromatograph (Metrohm Compact IC Plus 882) was used for the analysis of major ions (Na^+, K^+, Ca^{2+}, Mg^{2+}) in the samples. For making required standards, ICP multi-element standards with known concentrations were used. Average accuracy for the analysis was 2% with an average precision of 1%. Expected concentrations of the known samples were plotted against measured concentrations for the analysis of total alkalinity, major ions, dissolved silica, and it shows a positive correlation ($r^2 = 0.9996$), which confirms the accuracy and precision of the experiments.

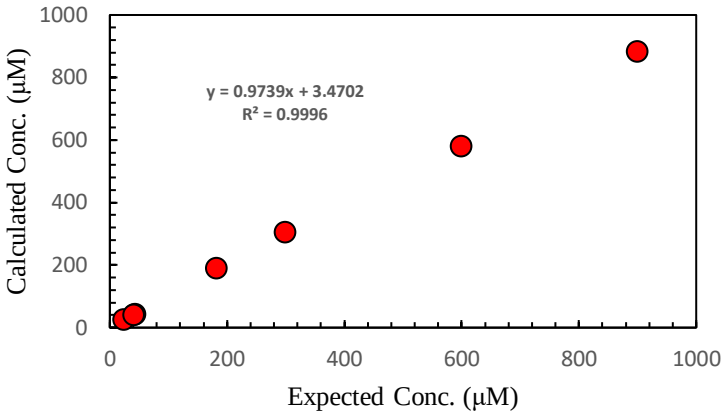

Figure 6: Plot of Calculated Concentration v/s Expected Concentration

2.2.2.3 Dissolved Silica

UV-VIS spectrophotometer was used for the measurement of the concentration of dissolved silica in the samples. The absorbance of the molybdenum-blue complexes formed by the samples were analysed by using 1 cm quartz cell at 700 nm wavelength. During the analysis, average accuracy of the measurements was 4% with a precision of 1%.

.

3. Chapter – 3

3.1 Results

Data of the major oxides of 30 rock samples have been provided in Table – 1. The concentration of SiO_2 ranges between 45.4 and 48.2 wt% (47.2 ± 0.5 wt%, n= 30), $FeO_{(T)}$ ranges between 15.9 and 17.2 wt% (16.4 ± 0.3 wt%, n = 30), Al_2O_3 ranges between 12.9 and 13.8 wt% (13.3 ± 0.2 wt%, n = 30), CaO ranges between 9 and 9.8 wt% (9.4 ± 0.2 wt%, n = 30), MgO ranges between 4.8 and 5.3 wt% (5.1 ± 0.1 wt%, n = 30), Na_2O ranges between 2.2 and 2.5 wt% (2.4 ± 0.1 wt%, n = 30), TiO_2 ranges between 2.1 and 2.6 wt% (2.3 ± 0.1 wt%, n = 30), K_2O ranges between 0.3 and 0.5 wt% (0.4 ± 0.04 wt%, n = 30), MnO ranges between 0.2 and 0.3 wt% (0.3 ± 0.01 wt%, n = 30), P_2O_5 ranges between 0.19 and 0.24 wt% (0.21 ± 0.01 wt%, n = 30). The obtained values align well with the published data (Laxman et al., 2022).

The average pH value of Milli-Q water used for this analysis is 5.8 ± 0.2 (n = 10).

Chemical data for total 25 leachate water samples have been provided in Table – 2. For leachate water samples collected after 1 hour, total alkalinity ranges between 84 and 180 µM (118 ± 43 µM, n = 5), Na^+ ranges between 58 and 105 µM (79 ± 24 µM, n = 5), Ca^{2+} ranges between 4 and 38 µM (17 ± 17 µM, n = 5), Mg^{2+} ranges between 4 and 7 µM (5 ± 1 µM, n = 5), SiO_2 ranges between 35 and 75 µM (54 ± 16 µM, n = 5).

For leachate water samples collected after 6 hours, total alkalinity ranges between 88 and 210 µM (141 ± 51 µM, n = 5), Na^+ ranges between 64 and 115 µM (86 ± 27 µM, n = 5), Ca^{2+} ranges between 5 and 44 µM (23 ± 17 µM, n = 5), Mg^{2+} ranges between 4 and 15 µM (7 ± 5 µM, n = 5), SiO_2 ranges between 34 and 115 µM (71 ± 31 µM, n = 5).

For leachate water samples collected after 12 hours, total alkalinity ranges between 97 and 230 µM (148 ± 54 µM, n = 5), Na^+ ranges between 67 and 121 µM (90 ± 28 µM, n = 5), Ca^{2+} ranges between 6 and 43 µM (23 ± 16 µM, n = 5), Mg^{2+} ranges between 4 and 18 µM (10 ± 6 µM, n = 5), SiO_2 ranges between 49 and 140 µM (94 ± 42 µM, n = 5).

For leachate water samples collected after 24 hours, total alkalinity ranges between 113 and 243 µM (165 ± 51 µM, n = 5), Na^+ ranges between 65 and 121 µM (90 ± 27 µM, n = 5), Ca^{2+} ranges between 26 and 49 µM (34 ± 11 µM, n = 5), Mg^{2+} ranges between 4 and 16 µM (9 ± 6 µM, n = 5), SiO_2 ranges between 60 and 142 µM (102 ± 38 µM, n = 5).

For leachate water samples collected after 48 hours, total alkalinity ranges between 114 and 269 µM (175 ± 64 µM, n = 5), Na^+ ranges between 65 and 131 µM (93 ± 30 µM, n = 5), Ca^{2+} ranges between 25 and 57 µM (37 ± 14 µM, n = 5), Mg^{2+} ranges between 4 and 20 µM (10 ± 8 µM, n = 5), SiO_2 ranges between 62 and 182 µM (120 ± 50 µM, n = 5).

3.2 Discussion

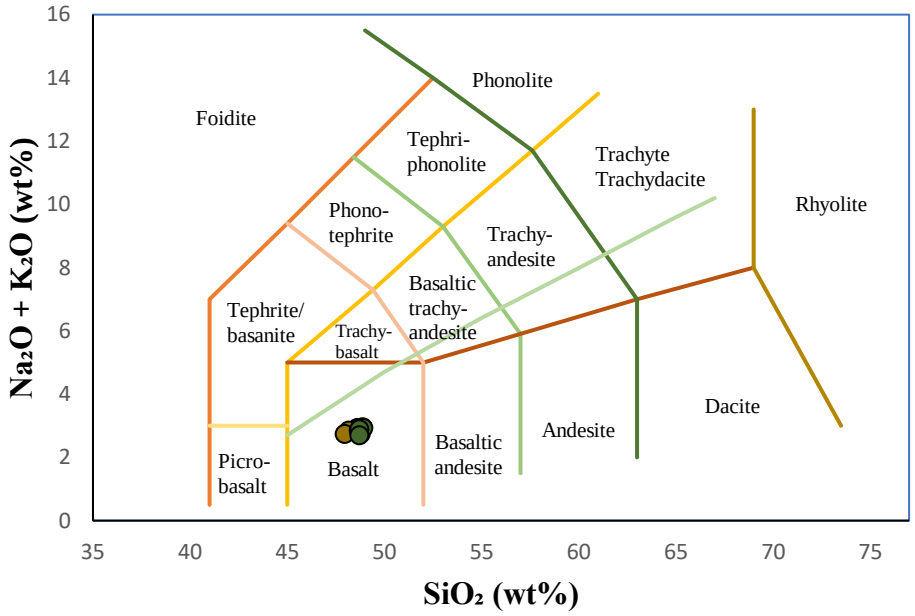

Figure 4: TAS diagram showing possible rock type (Le Bas et al., 1986)

To classify the rock samples according to their total alkali ($Na_2O + K_2O$) and silica (SiO_2) contents, data obtained from the XRF analysis were plotted in the TAS diagram (Figure - 4). The basalt field in the diagram contains all thirty samples. Significantly, every sample has a subalkaline affinity since they are all below the subalkaline–alkaline dividing line. Additionally, close grouping of the data points indicates that the samples are almost geochemically homogeneous. Therefore, it is confirmed that the rocks under study are subalkaline basaltic in nature.

For further classification with respect to the relative proportions of alkalis ($Na_2O + K_2O$), total iron (FeO*), and magnesium (M = MgO), data obtained for the respective major oxides for all samples were plotted in the AFM diagram (Figure – 5). All the plotted samples are grouped above the calc-alkaline boundary in the iron-enriched tholeiitic field, which confirms a tholeiitic fractionation trend.

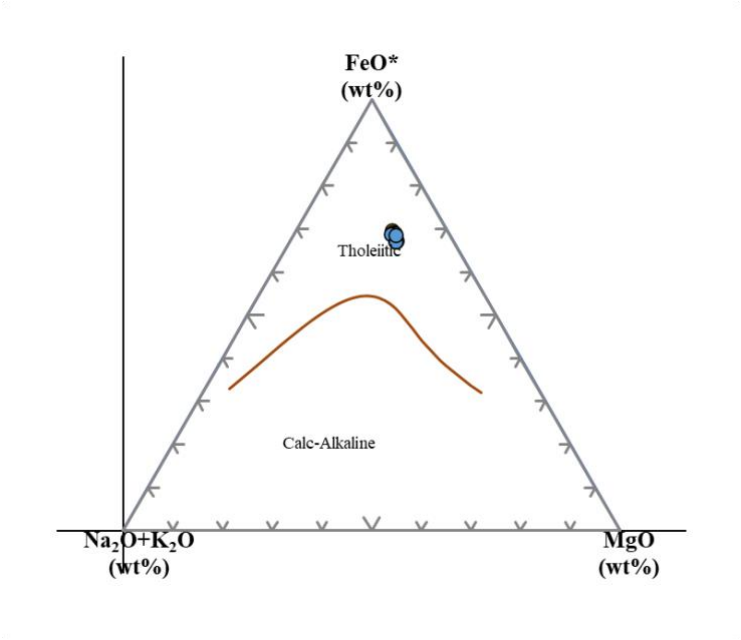

Figure 5: Plotting of the rock samples in AFM diagram (Irvine and Baragar, 1971)

So, all the basalt samples that were used to conduct the controlled experiment are subalkaline tholeiitic in nature. Major minerals in subalkaline tholeiitic basalt are olivine, orthopyroxene, clinopyroxene, and plagioclase feldspar (Winter, 2014). As these types of basalts are rich in Ca and Mg-bearing silicate minerals, they are well suited for the controlled experiment of carbon sequestration.

Natural rainwater has a pH of 5.6. To replicate this, Milli-Q water with an initial pH of 5.8 ± 0.2 was used in the controlled experiment conducted. The pH value of the Milli-Q water is a result of equilibration with atmospheric CO_2. Milli-Q water contains no background ions. This property allows for the accurate quantification of the concentration of cations released from the basalt powder and the exact measurement of alkalinity generated through the dissolution of basalt powder. So, the carbon sequestration potential of powdered basalt can be quantified precisely with this experiment.

The shaker was operated at 50 rpm for the controlled experiment. It ensures continuous mixing of the basalt powder with Milli-Q water at a gentle pace. This low to moderate shaking speed actually mimics low-energy hydrological conditions that are found in nature. The pace is enough to maintain the system mixing without being overly intense, which can overestimate the weathering rate.

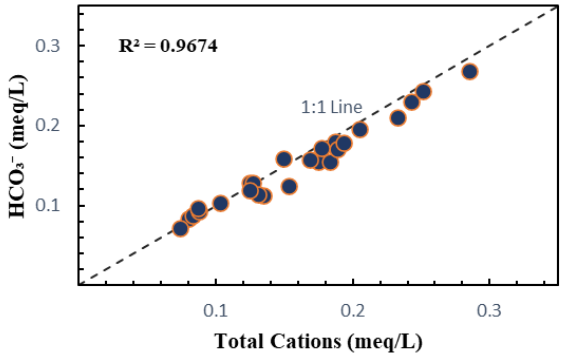

Figure 6: Plotting of HCO_3^- (meq/L) v/s Total Cations (meq/L) for leachate water samples of controlled experiment

If the equivalent ratio of total alkalinity and total cations is 1, then the process can be classified as silicate weathering (Roy & Sen, 2023). So, respective data obtained from the controlled experiment was plotted for all leachate water samples from different time points (Figure – 6). All data points almost follow a 1:1 line. The plot shows a positive linear correlation with an r^2 value of 0.9674, where the equivalent ratio of total cations and total alkalinity ranges from 0.90 to 1.22 with a mean value of 1.04 ± 0.08 (n = 25). This confirms that all of the ionic species that were detected in the leachate water samples generated through controlled experiment are products of the weathering of silicate minerals that were present in the basalt powder.

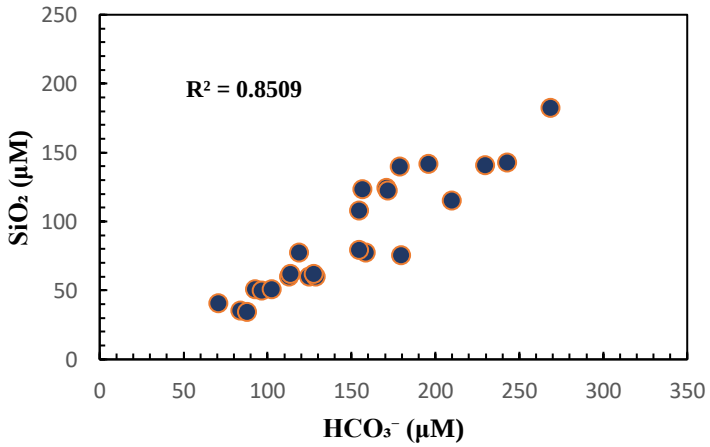

Figure 7: Plotting of SiO_2 (µM) v/s HCO_3^- (µM) for leachate water samples of controlled experiment

Concentration of SiO_2 and total alkalinity from the controlled experiment was plotted against each other for all leachate water samples from different time points (Figure – 7). The plot shows

a strong positive linear correlation with an r^2 value of 0.8509. This confirms that total alkalinity in the leachate water samples is mainly generated from the weathering of silicate minerals that were present in the basalt powder (Ghezzi et al., 2017).

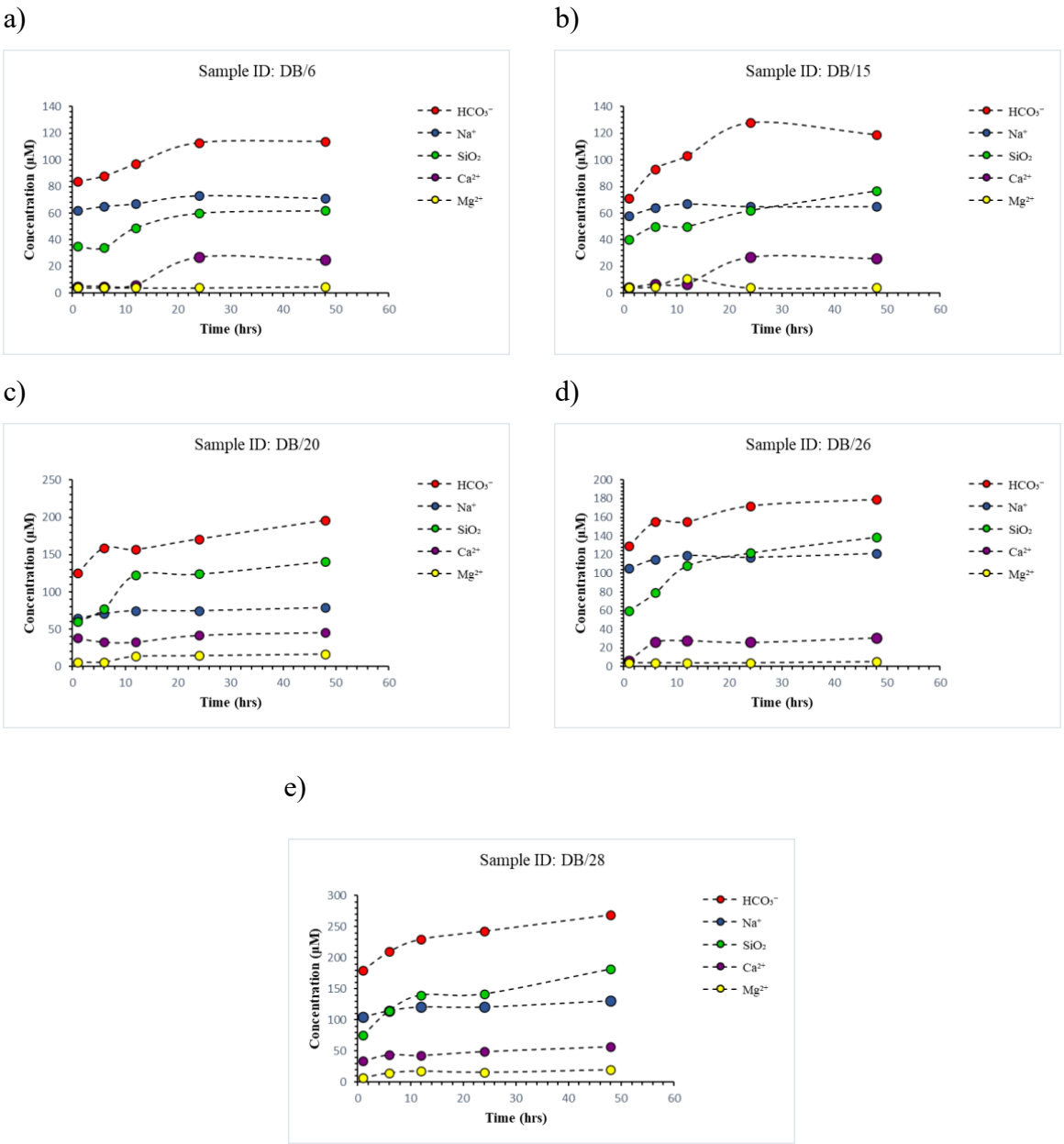

Figure 8: Plots showing changes of concentration of different species in the leachate water with time for different rock samples

Concentration of different elements in the leachate water samples for individual rock powders was plotted against time to observe the trends. Overall steady increasing trends with time were observed for total alkalinity and SiO_2 across all the samples, indicating active silicate

weathering. But the magnitude of the increment slightly decreases after 24 hours. This indicates exchangeable phases get leached during the early stages of the weathering.

Concentration of Na^+ shows a mild increasing trend during the very early stages of the weathering, and it gets stabilized very quickly, which is indicated by the flat plateau. Also, the concentration is much higher than Ca^{2+} and Mg^{2+} from the very beginning of the experiment. It suggests that Na^+ is an easily exchangeable phase in this scenario. According to Romano et al., 2024, the relative mobility of Na^+ is higher in the basalt-water-CO_2 interaction system. So, it can be the reason behind the higher concentration of Na^+. In the subalkaline tholeiitic basalt, the main source of Na^+ is plagioclase feldspar which is the dominant mineral phase within it according to modal mineralogy (Winter, 2014). So, it can be another reason behind the higher concentration of Na^+.

Enrichment in the concentration of Ca^{2+} in the leachate water samples is mainly observed after 6 hours. The increasing trend continues up to 24 hours, and after that, the graph is almost defined by a flat plateau. It suggests that Ca^{2+} does not get released easily during the very early stages of the weathering.

Throughout the experiment, Mg^{2+} showed a nearly stationary trend with constant low concentration. According to modal mineralogy, the main source of Mg^{2+} in subalkaline tholeiitic basalt is olivine and pyroxene. These minerals are highly reactive silicate phases (Lasaga, 1995). Still, Mg^{2+} is present in very low amounts in leachate water samples. It suggests that Mg^{2+} does not get released easily during the short duration of weathering. The relative mobility of Mg^{2+} is lower in the basalt-water-CO_2 interaction system (Romano et al., 2024). So, it can be the reason behind the lower concentration.

So, from all the observations, it can be concluded that in the basalt-water-CO_2 interaction system, the relative mobility of elements is $Na^+ > Ca^{2+} > Mg^{2+}$. Na^+ can be considered as an easily exchangeable phase in the context of silicate weathering. It supports previously reported studies (Flaathen et al., 2009; Romano et al., 2024).

The highest concentration of Na^+, Ca^{2+}, and Mg^{2+} in the leachate water samples has been observed around 24 hours to 48 hours, and there are not that many differences in concentration around these time points. So, by considering the concentration of these elements around these timepoints, carbon sequestration potential can be defined based on stoichiometry. According to

stoichiometry, 1 mol CO_2 is captured per mol of Mg^{2+} or Ca^{2+}, and 0.5 mol CO_2 is captured per mol of Na^{+} (Lewis et al., 2021).

So,

$$CO_2 \text{ uptake} \approx [Ca^{2+}] + [Mg^{2+}] + 0.5\,[Na^{+}]$$

By calculating from this equation, it has been observed that the carbon sequestration potential of 1g basalt powder approximately ranges between 0.193 mg CO_2/day and 0.439 mg CO_2/day with an average of 0.280 ± 0.085 mg CO_2/day (n = 10; for this calculation, data points from 48 hours have been approximated as 24 hours as very little variation in the concentration of desired elements between these time points has been observed due to early-stage closed-system weathering in ultrapure deionized medium).

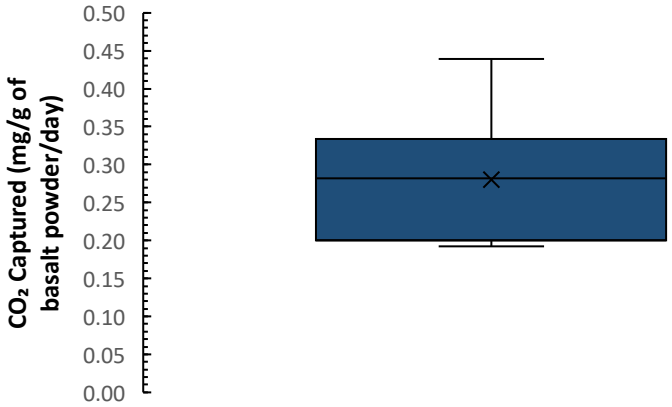

Figure 9: Graphical representation of carbon sequestration potential of basalt powder (n = 10)

4. Chapter – 4

4.1 Conclusion

The naturally occurring weathering cycle, which consumes CO_2 from the atmosphere, is a very slow process. Considering the scenario of increasing global warming, using EW as a CO_2 removal technique to mitigate climate change by accelerating the natural process of silicate mineral weathering can be a promising approach. It involves the spreading of finely powdered silicate rocks, particularly basalt over agricultural lands, and forest areas as this rock is easily available on the land surface. This study finds -

- interaction between finely powdered basalt, water, and CO_2 can sequester significant amounts of carbon (0.280 ± 0.085 mg CO_2/day/g of basalt powder) by increasing the total alkalinity of the medium and releasing major cations like Na^+, Ca^{2+}, and Mg^{2+}.
- Na^+ can be considered as an easily exchangeable phase in the context of silicate weathering.
- during this interaction, the relative mobility of elements is $Na^+ > Ca^{2+} > Mg^{2+}$.
- subalkaline tholeiitic basalt can be used for the application of EW as this type of basalt contains a significant amount of reactive minerals like plagioclase feldspar, pyroxene, and olivine.
- DVP being one of the most voluminous large igneous provinces, can provide a significant amount of capacity for mineral sequestration.

Detailed further study should be done to track the release of toxic metals like Cu and Ni during the interaction between basalt powder, water, and CO_2. Also, a mesocosm study with plants can be conducted to study the vegetation model coupled with the weathering model.

References

Amann, T., Hartmann, J., Struyf, E., de Oliveira Garcia, W., Fischer, E. K., Janssens, I., ... & Schoelynck, J. (2020). Enhanced Weathering and related element fluxes–a cropland mesocosm approach. *Biogeosciences*, *17*(1), 103-119.

Anda, M., Shamshuddin, J., & Fauziah, C. I. (2013). Increasing negative charge and nutrient contents of a highly weathered soil using basalt and rice husk to promote cocoa growth under field conditions. *Soil and Tillage Research*, *132*, 1-11.

Archer, D., Kheshgi, H., & Maier-Reimer, E. (1997). Multiple timescales for neutralization of fossil fuel CO2. *Geophysical Research Letters*, *24*(4), 405-408.

Beane, J. E., Turner, C. A., Hooper, P. R., Subbarao, K. V., & Walsh, J. N. (1986). Stratigraphy, composition and form of the Deccan basalts, Western Ghats, India. *Bulletin of Volcanology*, *48*, 61-83.

Berner, R. A., Lasaga, A. C., & Garrels, R. M. (1983). Carbonate-silicate geochemical cycle and its effect on atmospheric carbon dioxide over the past 100 million years. *Am. J. Sci.;(United States)*, *283*(7).

Brierley, A. S., & Kingsford, M. J. (2009). Impacts of climate change on marine organisms and ecosystems. *Current biology*, *19*(14), R602-R614.

Change, I. P. O. C. (2007). Climate change 2007: the physical science basis. *Agenda*, *6*(07), 333.

Chenet, A. L., Courtillot, V., Fluteau, F., Gérard, M., Quidelleur, X., Khadri, S. F. R., ... & Thordarson, T. (2009). Determination of rapid Deccan eruptions across the Cretaceous-Tertiary boundary using paleomagnetic secular variation: 2. Constraints from analysis of eight new sections and synthesis for a 3500-m-thick composite section. *Journal of Geophysical Research: Solid Earth*, *114*(B6).

Colleps, C. L., McKenzie, N. R., Guenthner, W. R., Sharma, M., Gibson, T. M., & Stockli, D. F. (2021). Apatite (U-Th)/He thermochronometric constraints on the northern extent of the Deccan large igneous province. *Earth and Planetary Science Letters*, *571*, 117087.

Conceição, L. T., Silva, G. N., Holsback, H. M. S., de Figueiredo Oliveira, C., Marcante, N. C., de Souza Martins, É., ... & Santos, E. F. (2022). Potential of basalt dust to improve soil fertility and crop nutrition. *Journal of Agriculture and Food Research*, *10*, 100443.

Courtillot, V. (1990). Deccan volcanism at the Cretaceous-Tertiary boundary: past climatic crises as a key to the future?. *Palaeogeography, Palaeoclimatology, Palaeoecology*, *89*(3), 291-299.

Doria, L. R. (2022). *Belvidere asbestos mine: site suitability for CO2 sequestration through mineral carbonation* (Doctoral dissertation, Middlebury).

Flaathen, T. K., Gislason, S. R., Oelkers, E. H., & Sveinbjörnsdóttir, Á. E. (2009). Chemical evolution of the Mt. Hekla, Iceland, groundwaters: A natural analogue for CO2 sequestration in basaltic rocks. *Applied Geochemistry*, *24*(3), 463-474.

Gale, J. (2004). Geological storage of CO2: What do we know, where are the gaps and what more needs to be done?. *Energy*, *29*(9-10), 1329-1338.

Gentzis, T. (2000). Subsurface sequestration of carbon dioxide—an overview from an Alberta (Canada) perspective. *International Journal of Coal Geology*, *43*(1-4), 287-305.

Ghezzi, L., Petrini, R., Montomoli, C., Carosi, R., Paudyal, K., & Cidu, R. (2017). Findings on water quality in Upper Mustang (Nepal) from a preliminary geochemical and geological survey. *Environmental Earth Sciences*, *76*, 1-13.

Gunter, W. D., Mavor, M. J., & Robinson, J. R. (2005). CO2 storage and enhanced methane production: field testing at Fenn-Big Valley, Alberta, Canada, with application. In *Greenhouse Gas Control Technologies 7* (pp. 413-421). Elsevier Science Ltd.

Hartmann, J., West, A. J., Renforth, P., Köhler, P., De La Rocha, C. L., Wolf-Gladrow, D. A., ... & Scheffran, J. (2013). Enhanced chemical weathering as a geoengineering strategy to reduce atmospheric carbon dioxide, supply nutrients, and mitigate ocean acidification. *Reviews of Geophysics*, *51*(2), 113-149.

Hilton, R. G., & West, A. J. (2020). Mountains, erosion and the carbon cycle. *Nature Reviews Earth & Environment*, *1*(6), 284-299.

Holland, H. D., Lazar, B., & McCaffrey, M. (1986). Evolution of the atmosphere and oceans. *Nature*, *320*(6057), 27-33.

Holloway, S. (2005). Underground sequestration of carbon dioxide—a viable greenhouse gas mitigation option. *Energy*, *30*(11-12), 2318-2333.

Honvault, N., Tiouchichine, M. L., Sauze, J., Piel, C., Landais, D., Devidal, S., ... & Milcu, A. (2024). Additive effects of basalt enhanced weathering and biochar co-application on carbon sequestration, soil nutrient status and plant performance in a mesocosm experiment. *Applied Geochemistry*, *169*, 106054.

Huijgen, W. J. J., & Comans, R. N. J. (2003). Carbon dioxide sequestration by mineral carbonation. Literature Review.

Jay, A. E., & Widdowson, M. (2008). Stratigraphy, structure and volcanology of the SE Deccan continental flood basalt province: implications for eruptive extent and volumes. *Journal of the Geological Society*, *165*(1), 177-188.

Kale, V. S., Dole, G., Shandilya, P., & Pande, K. (2020). Stratigraphy and correlations in Deccan Volcanic Province, India: quo vadis?. *GSA Bulletin*, *132*(3-4), 588-607.

Kelland, M. E., Wade, P. W., Lewis, A. L., Taylor, L. L., Sarkar, B., Andrews, M. G., ... & Beerling, D. J. (2020). Increased yield and CO2 sequestration potential with the C4 cereal Sorghum bicolor cultivated in basaltic rock dust-amended agricultural soil. *Global Change Biology*, *26*(6), 3658-3676.

Khosla, A., & Sahni, A. (2003). Biodiversity during the Deccan volcanic eruptive episode. *Journal of Asian Earth Sciences*, *21*(8), 895-908.

Knapp, W. J., Stevenson, E. I., Renforth, P., Ascough, P. L., Knight, A. C., Bridgestock, L., ... & Tipper, E. T. (2023). Quantifying CO2 removal at enhanced weathering sites: a multiproxy approach. *Environmental science & technology*, *57*(26), 9854-9864.

Lasaga, A. C. (1995). Fundamental approaches in describing mineral dissolution and precipitation rates. *Reviews in mineralogy*, *31*, 23-86.

Laxman, M. B., Nagaraju, B., Nagaraju, K., & Kumar, K. V. (2022). Spatial variations in the geochemical characteristics of basalts from the Deccan Volcanic Province, India: Role of mixing and assimilation fractional crystallisation. *Journal of Earth System Science*, *131*(3), 186.

Lewis, A. L., Sarkar, B., Wade, P., Kemp, S. J., Hodson, M. E., Taylor, L. L., ... & Beerling, D. J. (2021). Effects of mineralogy, chemistry and physical properties of basalts on carbon capture potential and plant-nutrient element release via enhanced weathering. *Applied Geochemistry*, *132*, 105023.

Luyckx, M., Hausman, J. F., Lutts, S., & Guerriero, G. (2017). Silicon and plants: current knowledge and technological perspectives. *Frontiers in plant science*, *8*, 411.

Metz, B., Davidson, O., De Coninck, H. C., Loos, M., & Meyer, L. (2005). *IPCC special report on carbon dioxide capture and storage*. Cambridge: Cambridge University Press.

Mun, M., & Cho, H. (2013). Mineral carbonation for carbon sequestration with industrial waste. *Energy Procedia*, *37*, 6999-7005.

Natasha, N., Shahid, M., Khalid, S., Bibi, I., Naeem, M. A., Niazi, N. K., ... & Rinklebe, J. (2022). Influence of biochar on trace element uptake, toxicity and detoxification in plants and associated health risks: A critical review. *Critical Reviews in Environmental Science and Technology*, *52*(16), 2803-2843.

Ozaki, M., Minamiura, J., Kitajima, Y., Mizokami, S., Takeuchi, K., & Hatakenaka, K. (2001). CO 2 ocean sequestration by moving ships. *Journal of Marine Science and Technology*, *6*, 51-58.

Park, A. H. A. (2005). *Carbon dioxide sequestration: Chemical and physical activation of aqueous carbonation of magnesium-bearing minerals and pH swing process*. The Ohio State University.

Renforth, P., von Strandmann, P. P., & Henderson, G. M. (2015). The dissolution of olivine added to soil: Implications for enhanced weathering. *Applied Geochemistry*, *61*, 109-118.

Richardson, J. B. (2024). Basalt Rock Dust Amendment on Soil Health Properties and Inorganic Nutrients—Laboratory and Field Study at Two Organic Farm Soils in New England, USA. *Agriculture*, *15*(1), 52.

Rigopoulos, I., Petallidou, K. C., Vasiliades, M. A., Delimitis, A., Ioannou, I., Efstathiou, A. M., & Kyratsi, T. (2015). Carbon dioxide storage in olivine basalts: effect of ball milling process. *Powder Technology*, *273*, 220-229.

Romano, P., Brusca, L., & Liotta, M. (2024). Element mobility during basalt-water-CO2 interaction: observations in natural systems vs. laboratory experiments and implication for carbon storage. *Geochemical Transactions*, *25*(1), 4.

Roy, N., & Sen, I. S. (2023). CO2 consumption rates in the glacierized Himalayan headwaters: The importance of sulfuric and nitric acid-mediated chemical weathering reactions in geologic carbon cycle. *Geochemistry, Geophysics, Geosystems*, *24*(7), e2023GC010919.

Sanna, A., Uibu, M., Caramanna, G., Kuusik, R., & Maroto-Valer, M. M. (2014). A review of mineral carbonation technologies to sequester CO 2. *Chemical Society Reviews*, *43*(23), 8049-8080.

Saran, R. K., Kumar, R., & Yadav, S. (2017). Climate change: mitigation strategyby various CO2 sequestration methods. *Int J Adv Res Sci Eng*, *6*, 299-308.

Schuiling, R. D., & De Boer, P. L. (2011). Rolling stones; fast weathering of olivine in shallow seas for cost-effective CO 2 capture and mitigation of global warming and ocean acidification. *Earth System Dynamics Discussions*, *2*(2), 551-568.

Schuiling, R. D., & Krijgsman, P. (2006). Enhanced weathering: an effective and cheap tool to sequester CO2. *Climatic Change*, *74*(1), 349-354.

Seifritz, W. (1990). CO2 disposal by means of silicates. *Nature*, *345*(6275), 486-486.

Sen, G. (2001). Generation of Deccan trap magmas. *Journal of Earth System Science*, *110*, 409-431.

Sloan Jr, E. D. (2003). Fundamental principles and applications of natural gas hydrates. *Nature*, *426*(6964), 353-359.

Subbarao, K. V., & Courtillot, V. (2017). Deccan basalts in and around Koyna—Warna region, Maharashtra: Some reflections. *Journal of the Geological Society of India*, *90*(6), 653-662.

Swoboda, P., Döring, T. F., & Hamer, M. (2022). Remineralizing soils? The agricultural usage of silicate rock powders: A review. *Science of The Total Environment*, *807*, 150976.

Taylor, L. L., Quirk, J., Thorley, R. M., Kharecha, P. A., Hansen, J., Ridgwell, A., ... & Beerling, D. J. (2016). Enhanced weathering strategies for stabilizing climate and averting ocean acidification. *Nature Climate Change*, *6*(4), 402-406.

Ten Berge, H. F., Van der Meer, H. G., Steenhuizen, J. W., Goedhart, P. W., Knops, P., & Verhagen, J. (2012). Olivine weathering in soil, and its effects on growth and nutrient uptake in ryegrass (Lolium perenne L.): a pot experiment.

Verma, O., & Khosla, A. (2019). Developments in the stratigraphy of the Deccan Volcanic Province, peninsular India. *Comptes Rendus Geoscience*, *351*(7), 461-476.

Vienne, A., Poblador, S., Portillo-Estrada, M., Hartmann, J., Ijiehon, S., Wade, P., & Vicca, S. (2022). Enhanced weathering using basalt rock powder: carbon sequestration, co-benefits and risks in a mesocosm study with Solanum tuberosum. *Frontiers in Climate*, *4*, 869456.

Voormeij, D. A., & Simandl, G. J. (2004). Geological, ocean, and mineral CO 2 sequestration options: a technical review. *Geoscience Canada*, *31*(1), 11-22.

Winter, J. D. (2014). *Principles of igneous and metamorphic petrology* (Vol. 2). Harlow, UK: Pearson education.

Zhang, D., Zeng, Q., Chen, H., Guo, D., Li, G., & Dong, H. (2024). Enhanced Rock Weathering as a Source of Metals to Promote Methanogenesis and Counteract CO2 Sequestration. *Environmental Science & Technology*, *58*(44), 19679-19689.

Annexure

Table – 1: Data of the major oxides of the rock samples

Sample ID	SiO_2	TiO_2	Al_2O_3	Fe_2O_3	MnO	MgO	CaO	Na_2O	K_2O	P_2O_5	LOI
	(wt%)										
DB/1	47.15	2.33	13.50	16.34	0.25	5.14	9.18	2.45	0.39	0.21	1.18
DB/2	47.08	2.27	13.33	16.01	0.27	5.09	9.62	2.35	0.31	0.21	1.65
DB/3	46.98	2.34	13.04	15.97	0.26	5.11	9.72	2.27	0.36	0.21	1.17
DB/4	47.07	2.31	13.24	16.28	0.24	4.98	9.63	2.41	0.37	0.20	1.15
DB/5	47.69	2.36	13.45	16.45	0.23	5.08	9.16	2.48	0.42	0.21	0.96
DB/6	47.33	2.31	13.54	16.31	0.25	5.20	9.33	2.44	0.38	0.20	1.52
DB/7	48.13	2.29	13.40	16.43	0.24	5.20	9.44	2.45	0.37	0.20	1.48
DB/8	47.13	2.25	13.46	16.20	0.24	5.20	9.43	2.44	0.37	0.19	1.90
DB/9	46.61	2.28	13.20	16.36	0.24	5.00	9.68	2.29	0.35	0.20	2.07
DB/10	47.72	2.34	13.31	16.36	0.25	5.15	9.49	2.44	0.36	0.20	1.59
DB/11	47.32	2.28	13.46	16.20	0.25	5.17	9.41	2.43	0.35	0.20	1.84
DB/12	46.85	2.49	12.94	17.17	0.27	4.77	9.19	2.34	0.40	0.22	1.30
DB/13	48.24	2.38	13.21	16.65	0.25	5.26	9.52	2.49	0.41	0.22	1.00
DB/14	47.11	2.40	13.18	16.73	0.24	4.92	9.40	2.31	0.39	0.21	0.86
DB/15	46.95	2.42	13.01	17.00	0.23	4.83	9.50	2.32	0.40	0.22	0.97
DB/16	46.52	2.31	13.08	16.44	0.26	5.21	9.79	2.40	0.35	0.21	0.83
DB/17	45.43	2.25	12.93	16.42	0.25	4.79	9.78	2.21	0.37	0.20	1.62
DB/18	47.56	2.43	13.44	16.35	0.24	5.08	9.23	2.47	0.49	0.21	0.86
DB/19	46.96	2.27	13.17	16.49	0.25	5.01	9.36	2.25	0.38	0.21	1.22
DB/20	47.45	2.41	13.28	16.33	0.25	5.03	9.46	2.28	0.39	0.22	0.75
DB/21	47.35	2.45	13.28	16.52	0.26	5.00	9.40	2.41	0.34	0.22	1.59
DB/22	47.55	2.58	12.98	16.86	0.26	4.77	9.10	2.42	0.41	0.24	1.49
DB/23	47.28	2.28	13.55	16.16	0.23	5.15	9.39	2.43	0.35	0.20	1.41
DB/24	47.14	2.40	13.19	16.53	0.28	4.95	9.40	2.24	0.36	0.22	3.44
DB/25	47.24	2.45	13.33	16.82	0.25	5.06	8.95	2.41	0.41	0.22	1.11
DB/26	47.50	2.38	13.28	16.54	0.25	5.24	9.53	2.42	0.36	0.21	2.37
DB/27	47.71	2.14	13.77	15.92	0.26	5.17	9.32	2.48	0.37	0.21	1.48
DB/28	46.70	2.33	13.03	16.35	0.27	4.99	9.37	2.37	0.36	0.21	1.44
DB/29	46.53	2.37	13.09	16.66	0.23	4.96	9.49	2.33	0.53	0.21	1.40
DB/30	47.38	2.26	13.25	16.00	0.26	5.05	9.38	2.22	0.37	0.21	1.95

Table – 2: Chemical data for leachate water samples

Sample ID	Time	HCO_3^-	SiO_2	Na^+	Ca^{2+}	Mg^{2+}
		(µM)				
DB/6		84	35	62	5	4
DB/15		71	40	58	4	4
DB/20		125	60	65	38	6
DB/26	1 hr.	129	60	105	6	4
DB/28		180	75	105	34	7
Mean		118	54	79	17	5
Std. Dev.		43	16	24	17	1
DB/6		88	34	65	5	4
DB/15		93	50	64	7	5
DB/20		159	77	71	33	6
DB/26	6 hrs.	155	79	115	26	4
DB/28		210	115	115	44	15
Mean		141	71	86	23	7
Std. Dev.		51	31	27	17	5
DB/6		97	49	67	6	4
DB/15		103	50	67	7	11
DB/20		157	123	75	33	14
DB/26	12 hrs.	155	108	119	28	4
DB/28		230	140	121	43	18
Mean		148	94	90	23	10
Std. Dev.		54	42	28	16	6
DB/6		113	60	73	27	4
DB/15		128	62	65	27	4
DB/20		171	124	75	42	15
DB/26	24 hrs.	172	122	117	26	4
DB/28		243	142	121	49	16
Mean		165	102	90	34	9
Std. Dev.		51	38	27	11	6
DB/6		114	62	71	25	5
DB/15		119	77	65	26	4
DB/20		196	141	79	46	17
DB/26	48 hrs.	179	139	121	31	5
DB/28		269	182	131	57	20
Mean		175	120	93	37	10
Std. Dev.		64	50	30	14	8